SUPPORTING INFORMATION

Winding-Locked Carbon Nanotubes/Polymer Nanofibers Helical Yarn for Ultra-Stretchable Conductor and Strain Sensor

Yuan Gao,[1,‡] Fengyun Guo,[2,‡] Peng Cao,[3] Jingchong Liu,[1] Dianming Li,[1] Jing Wu[4], Nü Wang,[1,] Yewang Su,[5,*] Yong Zhao[1,*]*

[1]Key Laboratory of Bioinspired Smart Interfacial Science and Technology of Ministry of Education, Beijing Key Laboratory of Bioinspired Energy Materials and Devices, School of Chemistry, Beijing Advanced Innovation Center for Biomedical Engineering, Beihang University, Beijing 100191, P. R. China.

[2]Key Laboratory of Advanced Textile Materials and Manufacturing Technology of Ministry of Education, College of Materials and Textiles, Zhejiang Sci-Tech University, Hangzhou 310018, China.

[3]College of Architecture and Civil Engineering, Beijing University of Technology, Beijing 100190, P. R. China.

[4]Beijing Engineering Research Center of Textile Nanofiber, Beijing Key Laboratory of Clothing Materials R&D and Assessment, School of Materials Design and Engineering, Beijing Institute of Fashion Technology, Beijing, 100029, P. R. China.

[5]State Key Laboratory of Nonlinear Mechanics, Institute of Mechanics, Chinese Academy of Sciences, Beijing 100190, China. School of Engineering Science, University of Chinese Academy of Sciences, Beijing 100049, China.

[‡]These two authors contributed equally to this work.

Corresponding [*]E-mail: zhaoyong@buaa.edu.cn, yewangsu@imech.ac.cn, wangn@buaa.edu.cn.

In this Supporting Information, we present a brief description of the winding-locked carbon nanotubes (CNTs)/ polyurethane (PU) helical yarn to characteristic its morphology and investigate the mechanical and conductive properties. There are sixteen figures in Supporting Information. First, we extend the morphology of pure PU oriented fibrous, yarn and helical yarn in Figure S1. The mechanical characteristic of CNTs/PU helical yarn are introduced in Figure S2-S5. From Figure S6 to S9, we display the electrical properties of the CNTs/PU yarn under deformation and then we discuss the mechanism of morphology and electrical resistance recoverability in Figure S10-S12. To further investigate the application of CNTs/PU helical yarn, Figure S13-S15 provide detailed performance of CNTs/PU yarn as a strain sensor. Finally, the general strategy to combination of different conductive materials with polymer substrates are summarized in Figure S16.

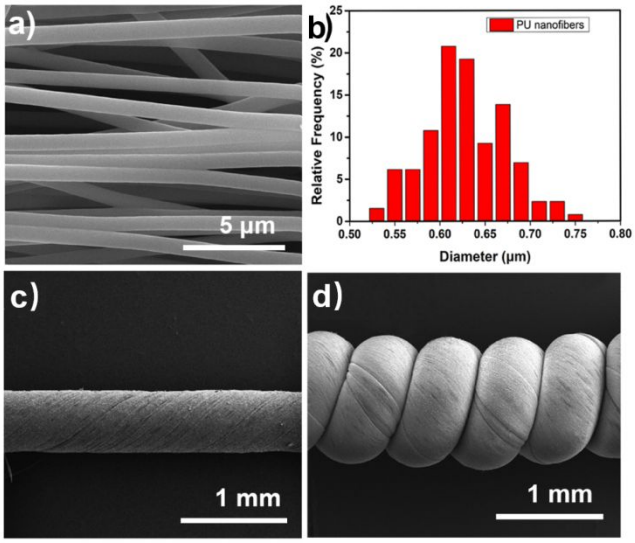

Figure S1. The SEM of a) PU oriented fibrous, b) diameter distribution of PU nanofibers, c) twisted PU yarn and d) helical PU yarn. The SEM of aligned PU nanofibers, twisted yarn and helical yarn without CNTs coating demonstrated the hierarchical structure of the pure PU helical yarn.

Through the electrospinning technology, the PU nanofibers were received by a roller to form a membrane. The PU nanofibers was oriented along the axis and the surface of them were highly smooth. The diameter of the nanofibers were uniform at 622.6±44.9 nm.

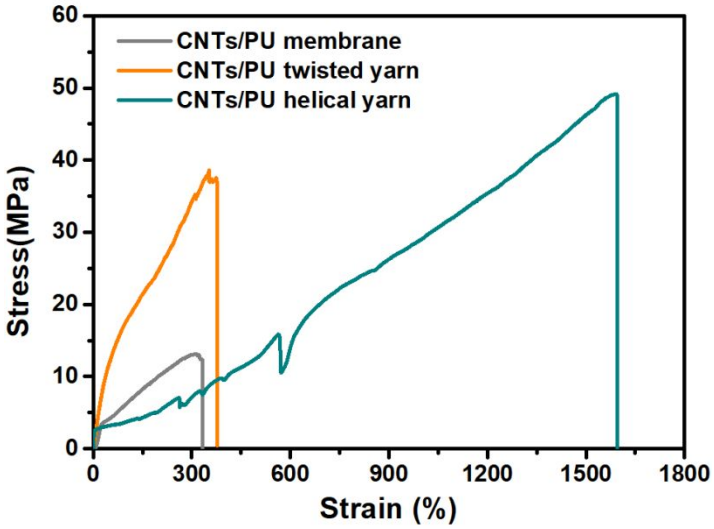

Figure S2. The mechanics curves of CNTs/PU film, CNTs/PU twisted yarn and CNTs/PU helical yarn. With the optimization of material structure, the fracture strength and breaking elongation have been improved which are consistent with the results displaying in Figure 2c.

The fracture strength of the CNTs/PU membrane, straight yarn and helical yarn were 13.1 ± 0.3 MPa, 40.1 ± 1.4 MPa and 50.2 ± 1.4 MPa respectively. After the coating of CNTs, the fracture strength of the membrane and fibers were increased 5 - 10 MPa comparing with pure PU materials, but the breaking elongation presented a slight drop.

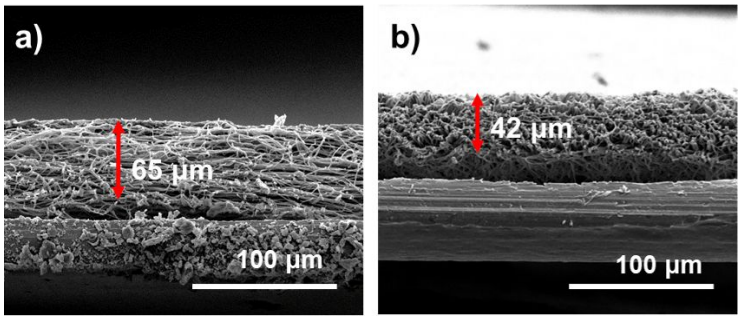

Figure S3. The cross section SEM of a) the PU film, b) EtOH treated PU film. With a more tightly stacked nanofibers, the thickness of PU film decreased after the evaporation of ethanol.

When the ethanol which soaked into the PU nanofiber membrane evaporated, the thickness of the PU membrane became thinner. This is mainly caused by that capillary force between the PU nanofibers was stronger and the nanofibers were more tightly stacked.

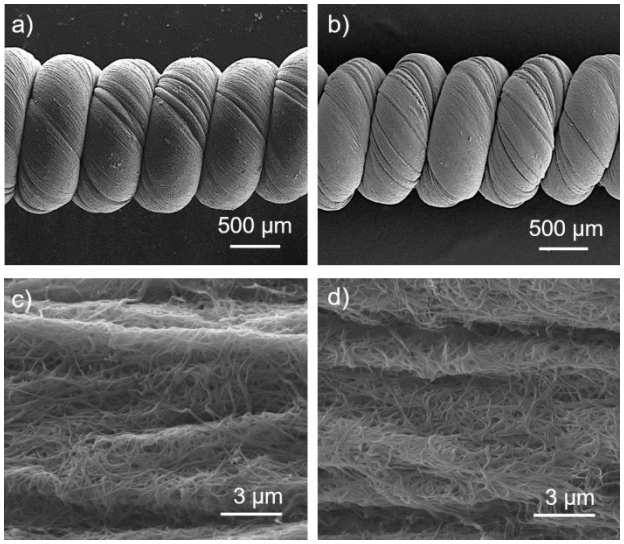

Figure S4. SEM images of the CNTs/PU helical yarn a) before and b) after 100 cycles with 100% stretching, the CNTs network c) before stretching, d) after 100 cycles. The structure of the helical yarn and the conductive CNTs networks have shown no change under 100% strain after 100 cycles.

The morphology of the helical yarn and CNTs before (Figure S4a, c) and after 100 cycles (Figure S4b, d) were conducted to further confirm the stability. After stretching cycles, CNTs conductive network remains integrity and the winding CNTs are tightly stacked without exfoliation due to the excellent stability of the helical structure and the winding-locked CNTs.

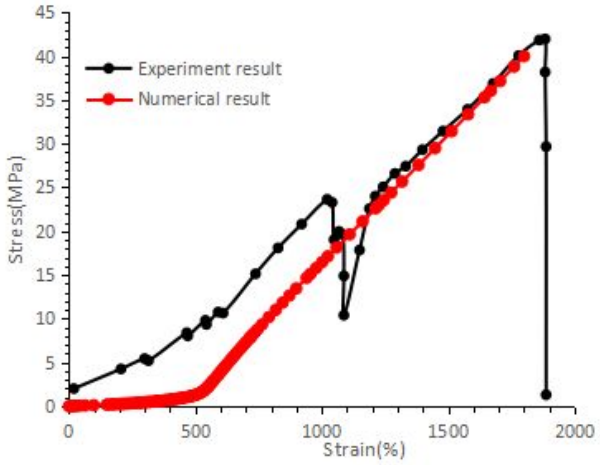

Figure S5. The experiment stress-strain curve and simulate stress-strain curve. In theory, helical yarn can withstand an ultra-large stain. The simulation result of mechanical stress agrees with the experimental result in Figure 2f.

To further clarify the stress changes of the helical structure under tension, the stress-strain data during the tension process were added in Figure S5. The stress/strain is defined as the nominal stress/nominal strain in the tensile direction, i.e.

Stress = reaction force / helical cross-sectional area

Strain = stretched length / original length

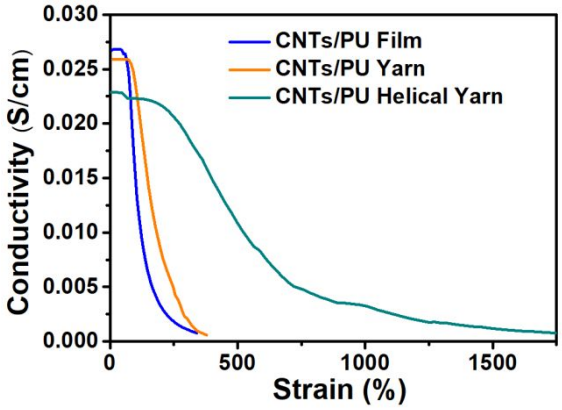

Figure S6. The conductivity change during stretching the film, straight yarn and helical yarn to break. CNTs/PU helical yarn displayed a relatively small conductivity variation under 400% stretching which verified the stability of the helical yarn.

The conductivity of the CNTs/PU membrane and CNTs/PU straight yarn were decreased non-linear with the increased strain. Compared with normal membrane material and twisting yarn, the conductivity variation of the helical over-twisted yarn was comparatively small in the first 400% stretching process, and then the tendency of the decreased resistance was same as twisting straight yarn.

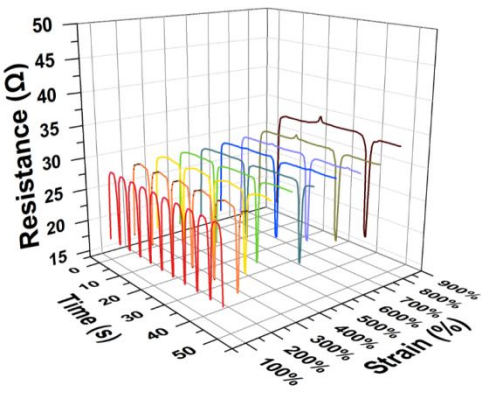

Figure S7. The resistance cyclic curves during different stretching-recovering processes from 100% to 900%. CNTs/PU helical yarn had a high resistance repeatability under 900% tensile strain.

According to the resistance curves, we can clearly see that the variation presented regular peaks and troughs curves at different strain and the resistance of the trough points were identical with the original resistance. It confirmed that the resistance of the helical CNTs/PU fiber has a preferable recoverability even at a large tensile strain.

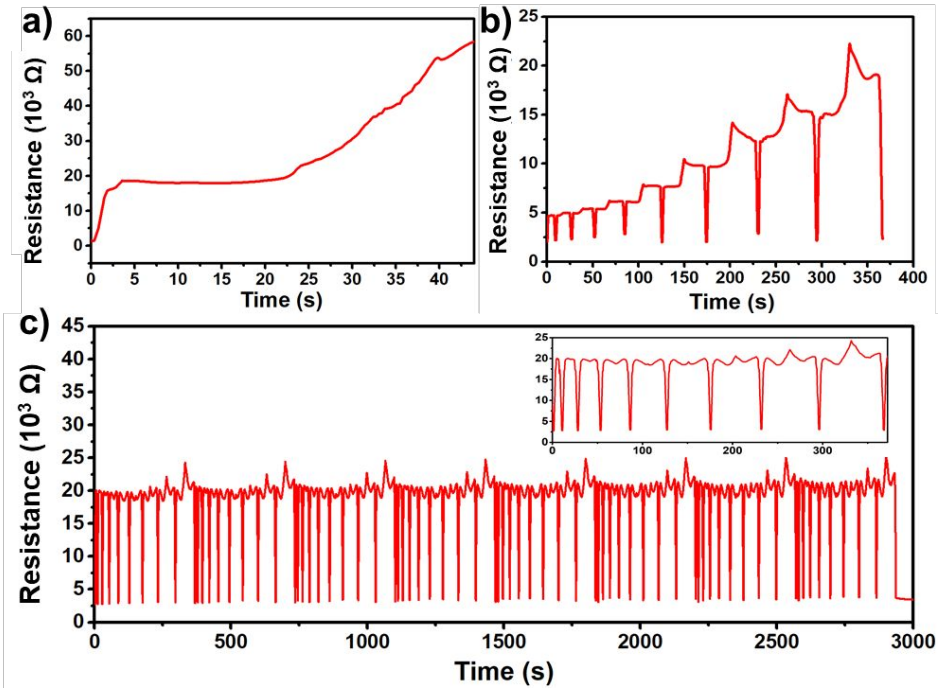

Figure S8. The CNTs coating on the twisted PU yarn, then overtwisted the yarn to get the helical yarn as a contrast sample. a) The conductivity change with the shifty strain. b) The first cycle of the stretching-recovering curve when the strain is gradually increased by every 100%. c) The cyclic curve before straighten the helical yarn, the inset is the enlarged picture of one set of the circle. Compared with the helical yarn which the CNTs coating on the both side of the PU film, the contrast sample shown poor structure and electrical stability.

As the conductive CNTs were only coated on the surface of the PU yarn, the conductive network of CNTs was unstable during the stretching process, and the adhesion between the CNTs and PU nanofibers was weakened, thus the resistance change stability was weakened.

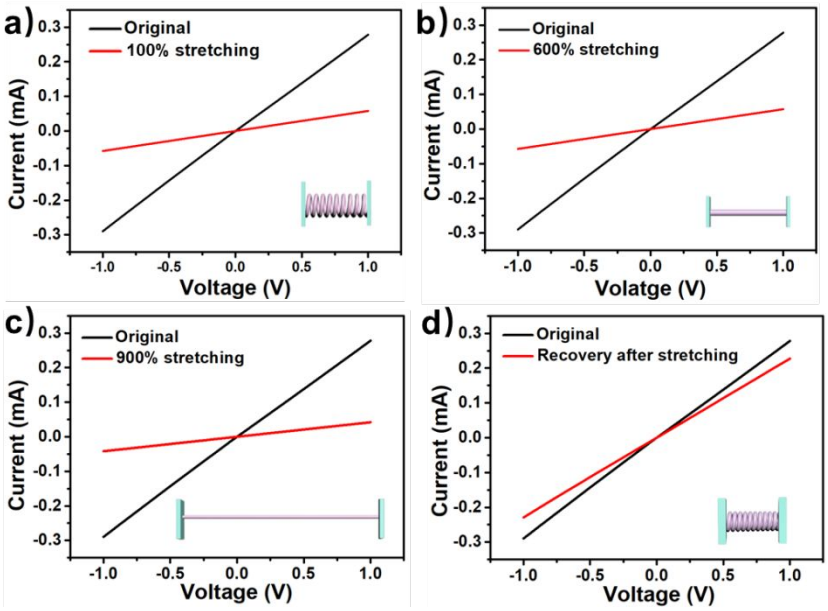

Figure S9. The voltage-current curves of the a) open the helical structure (100% stretching), b) straighten the helical fiber to the straight fiber (600% stretching), c) stretch the 1D fiber (900%) and d) recover to the initial state. The electrical resistance cannot recover to original state after the helical yarn recovery after stretching.

The current-voltage curves of the contrast sample before and after tensile have an obvious variation. The resistance change during the stretch-recover cycle test presented a slightly less stability and recoverability than CNTs/PU yarn. These can be proven that the conductive network inside the helical yarn played a very important role in maintaining the electrical stability with the fiber deformation.

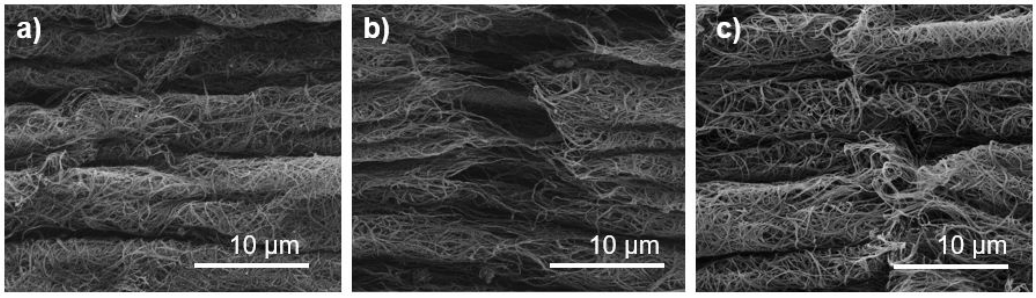

Figure S10. The SEM of the a) original state, b) 900% stretching state, c) recovery state after 900% stretching. The conductive network can be re-lapped while the helical structure recovered after releasing the stretching.

Once the helical yarn was turned straight, continue to stretch the fiber, the CNTs will be snapped, the surface of the CNTs network will appear small cracks. But under 900% stretching, these cracks can be rejoined when the yarn return to the helical structure.

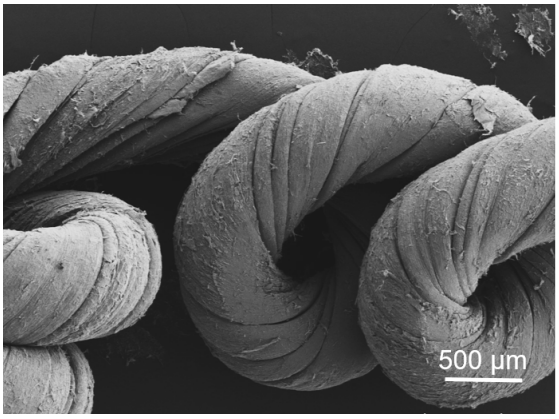

Figure S11. SEM image of tangled CNTs/PU yarn after suffering the 1300% strain. It is seen the helical structure cannot recover and the CNTs on the fibers surface exfoliated.

With an over-large stretching deformation, the straight yarn becomes thinner. After stretch releasing, the helical structure is overrelaxed and can't be recovered. As the Figure S11 shown, the spiral loops are loose and unordered.

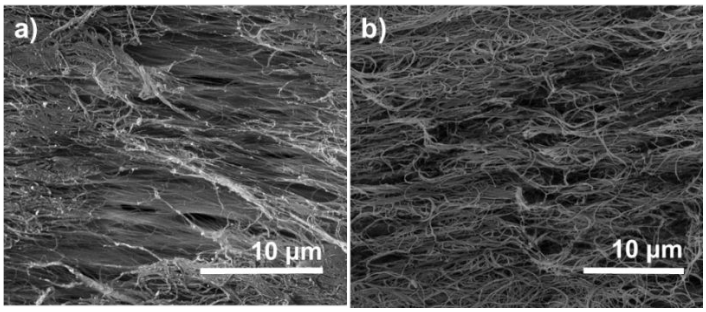

Figure S12. The SEM of the a) 1100% stretching state, b) recovery state after 1100% stretching. The conductive network cracked irreversibly under an ultra-large stretching.

Making a further stretch to the yarn, many cracks on CNTs network connected with each other to form a chasm. The surface of the CNTs in some places developed to a conductive-nonconductive-conductive distribution. The electron transport path will be cut in part of the area. And now the structure can't be recovered to the helical state, so the resistance shown the nonlinear increased tendency with the following stretch.

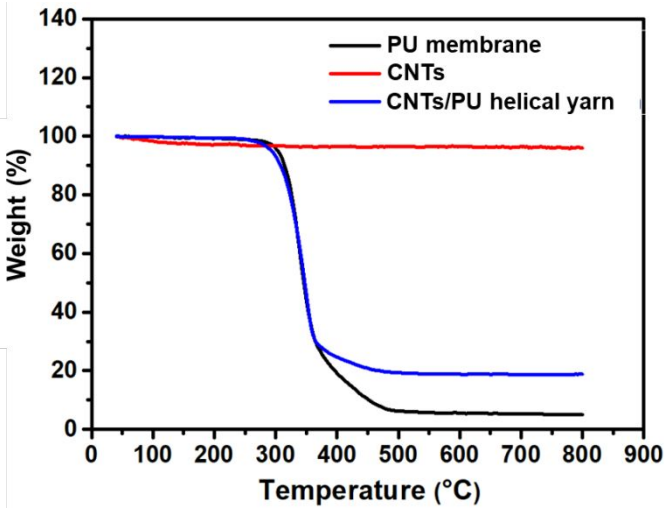

Figure S13. The thermogravimetric results of the PU film, CNTs and CNTs/PU helical yarn. CNTs accounted for about 11.7% of the CNTs/PU helical yarn as the strain sensor.

While in Figure 5, the helical CNTs/PU yarn was used as a strain sensor, which didn't requires a low resistance, but a better sensitivity, resistance recoverability. By reducing the doping amount of CNTs, we can adjust the conductivity and strain sensitivity of the helical yarn.

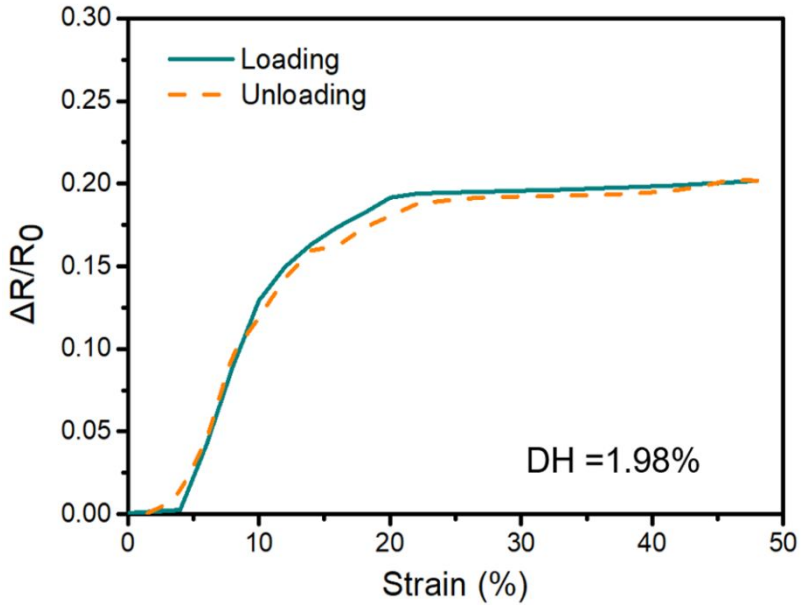

Figure S14. Hysteresis curve of the CNTs/PU helical yarn. The degree of hysteresis (DH) was 1.98%. The relatively low value of DH demonstrated the fast electrical response of the CNTs/PU helical yarn.

According to the formula,

$$DH = \frac{A_{loanding} - A_{unloanding}}{A_{loanding}} \times 100\%$$

where $A_{Loading}$ and $A_{Unloading}$ are the area of loading and unloading curves, respectively. A lower degree of hysteresis (DH) value indicates lesser hysteresis in the electrical response. The DH value of the CNTs/PU helical yarn was about 1.98%. The CNTs/PU helical yarn sensor exhibited a

negligible difference in the resistance responses between the loading and unloading curves, highlighting its hysteresis-free property and deterministic sensing performance.

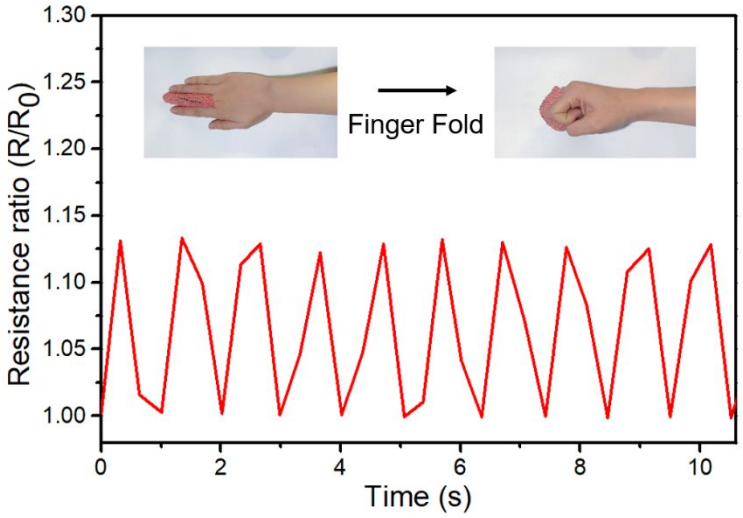

Figure S15. The CNTs/PU helical yarn was woven into a woolen fingerstall. Application of CNTs/PU helical yarn as strain sensor to monitor the resistance changes during finger folding. It exhibited stable resistance repeatability for human motions and has a great potential applications in the field of wearable sensors.

We weaved the prepared CNTs/PU helical yarn into a fingerstall to ensure that the yarn could contact and monitor the deformation of the finger folding. The real-time movement curve which shows excellent repeatability of resistance has similar variation trend with the demonstration in Figure 5. Owing to the low-cost, flexible and knittable features of CNTs/PU helical yarn, it is competent to be woven into fabric and used as a wearable sensor.

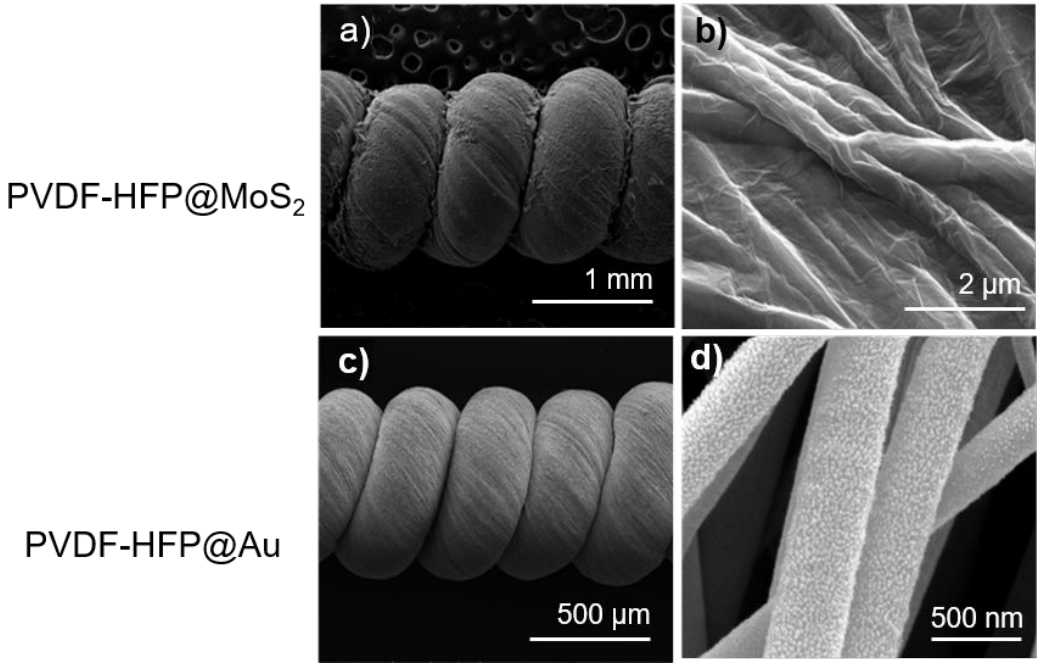

Figure S16. The combination of different host materials and guest materials. a) The SEM of the PVDF-HFP@MoS_2 helical yarn, b) the high magnification SEM of the MoS_2 which covered on the PVDF-HFP nanofibers to form a conductive film, c) the SEM of the PVDF-HFP@Au helical yarn, d) the high magnification SEM of the PVDF-HFP nanofibers which coated by tightly packed Au nanoparticle. Various conductive helical yarn can be fabricated by compounding different host materials and conductive guest materials.

We can selected different electrospun polymers as substrates and then coated different one-dimensional and two-dimensional conductive materials on their surface. Our investigations provide a general strategy to fabricate the stretchable and wearable conductor and strain sensor.